A novel defect in mitochondrial p53 accumulation following DNA damage confers apoptosis resistance in Ataxia Telangiectasia and Nijmegen Breakage Syndrome T-cells

A NOVEL DEFECT IN MITOCHONDRIAL P53 ACCUMULATION FOLLOWING DNA DAMAGE CONFERS APOPTOSIS RESISTANCE IN ATAXIA TELANGIECTASIA AND NIJMEGEN BREAKAGE SYNDROME T-CELLS

Valentina Turinetto[a], Paola Porcedda[a], Valentina Minieri[a], Luca Orlando[a], Erica Lantelme[a], Lisa Accomasso[a], Antonio Amoroso[b], Mario De Marchi[a], Laura Zannini[c], Domenico Delia[c], Claudia Giachino[a]

[a]Department of Clinical and Biological Sciences, University of Turin, Italy; [b]Department of Genetics, Biology and Biochemistry, University of Turin, Italy; [c]Department of Experimental Oncology, Fondazione IRCCS Istituto Nazionale Tumori, Milan, Italy.

Corresponding Author: Claudia Giachino, Department of Clinical and Biological Sciences, University of Turin, Italy: Regione Gonzole 10, 10043 Orbassano (Turin), Italy; Phone +390116705425; Fax +390119038639; e-mail claudia.giachino@unito.it

Abbreviations

ActD, Actinomycin D

AT, Ataxia Telangiectasia

DSB, DNA double-strand break

IR, ionizing radiation

LMB, leptomycin B

NBS, Nijmegen Breakage Syndrome

α-PFT, α pifithrin

μ-PFT, μ pifithrin

PI, propidium iodide

Abstract

We have previously shown that whereas T-cells from normal individuals undergo accumulation of p53 and apoptosis when treated with the genotoxic agent Actinomycin D (ActD), those from Ataxia Telangiectasia (AT) and Nijmegen Breakage Syndrome (NBS) patients resist ActD-induced apoptosis [1]. We have now found similar resistance by the p53-null Jurkat T-cell line and by siRNA p53-knockdown normal T-cells. This evidence that ActD initiates a p53-dependent apoptotic responce prompted us to look for defective p53 accumulation by AT and NBS T-cells. Surprisingly the total p53 level was only slightly reduced compared to normal T cells but its intracellular localization was highly defective: p53 was poorly accumulated in the cytosol and nearly undetectable in mitochondria. In accordance with the dependence of ActD-induced apoptosis on a mitochondrial p53 function, in control T-cells specific inhibition of mitochondrial p53 translocation with μ pifithrin reduced apoptosis by 86%, whereas treatment with α pifithrin, which blocks p53-mediated transcription, had no effect. We also showed that nuclear export is not required for mitochondrial p53 translocation. Observation of an altered p53 ubiquitination pattern and Mdm2 accumulation in ActD-treated AT and NBS T-cells provided a mechanistic link to their defective extranuclear p53 localization.

Our results disclose an undescribed defect in mitochondrial p53 accumulation in AT and NBS T-cells that makes them resistant to apoptosis following unrepairable DNA damage.

Keywords

Ataxia Telangiectasia

Nijmegen Breakage Syndrome

p53

apoptosis

DNA damage

1. Introduction

DNA damage-induced apoptosis and precise DNA repair are critical cellular function, and both are needed to prevent cancer [2-6]. Defective apoptosis contributes to mutagenesis, carcinogenesis, and the resistance of cancer cells to a variety of therapeutic agents [6]. DNA damage-induced apoptosis involves the participation of several factors with both overlapping and distinct functions, that are largely mediated by p53) [7, 8]. In conditions of genotoxic stress, the increased abundance of p53 orchestrates multiple responses that involve both transcription-dependent and transcription-independent mechanisms [9]. In the nucleus, p53 acts as a transcription factor to induce pro-apoptotic and/or cell cycle arresting programs by transactivating genes encoding pro-apoptotic and/or negative regulators of cell cycle progression [10]. Additionally, a direct apoptotic role of the p53 protein at the mitochondrial compartment in response to genotoxic stress has been amply demonstrated [11, 12]. Mitochondrial p53 participates in the intrinsic apoptosis pathway by interacting with members of the Bcl-2 family to induce mitochondrial outer membrane permeabilization, thereby triggering the release of pro-apoptotic factors from the mitochondrial intermembrane space [13, 14]. p53 turnover is regulated by Mdm2, which binds p53 and functions as an ubiquitin E3 ligase to promote its degradation by the proteasome [15, 16]. It mediates both poly- and mono-ubiquitylation of p53, and while abundant levels of Mdm2 promote p53 poly-ubiquitylation and degradation, limiting levels of Mdm2 promote p53 mono-ubiquitylation on one or few lysines [17].

ATM and NBS1 proteins are key regulators of the DNA damage response. ATM is a central component of the signal transduction pathway activated by DNA double-strand breaks (DSBs), and synchronizes DNA repair with the induction of p53-dependent apoptosis [4, 18]. Individuals who inherit germline ATM mutations on both alleles develop AT, a disorder characterised by progressive neurodegeneration and predisposition to the development of lymphoid malignancies [19, 20]. The cellular consequences of ATM dysfunction include chromosomal radiosensitivity, radioresistant DNA synthesis, loss of cell cycle checkpoints, and p53 dysfunction [18]. NBS1 acts by forming a complex with RAD50/MRE11 and by activating ATM. It is mutated in the NBS and cell lines derived from NBS patients display hypersensitivity to ionizing radiation (IR), chromosome instability, and defects in cell cycle checkpoint following DNA damage [20, 21]. The direct interconnection of ATM and NBS1, e.g. ATM phosphorylates NBS1 and NBS1 in turn is required for full ATM activation [22-24] accounts for the common pathogenetic mechanisms and the similar cellular and clinical phenotype of AT and NBS [20, 25, 26].

ActD is an anti-tumour antibiotic used in many chemotherapeutic protocols [27-29]. It intercalates into DNA and interferes with RNA polymerases and DNA topoisomerases, thus inhibiting

transcription and inducing various types of DNA damage [30-32], including DSBs [1]. This multiplicity of action is shared with many other genotoxic agents such as cisplatin and the topoisomerase I inhibitor camptothecin [33-35].

We have previously reported a defective p53 accumulation following IR in AT and NBS cells [36-39] and, like others, foud that DSBs in these cells are not completely repaired [1, 40]. Nevertheless, these residual DSBs did not induce apoptosis in patients's quiescent cells, as also confirmed by our ongoing studies on genomic stability in T cells. Thus, the mechanism of radiation induced response is well defined in patients' cells [41] at least to the point of accounting for the radiosensitivity of proliferating cells vs the characteristic radioresistence of quiescent cells. In contrast, we have shown that ActD treatment induces an accumulation of unrepairable DSBs and high amounts of total p53, followed by apoptosis in normal T-cells but not T cells from AT and NBS patients were resistant [1]. In this case, both the mechanism of p53 activity after ActD treatment and the underlying resistance of AT and NBS cells are still unknown.

Here we show that ActD-induced apoptosis depends on a mitochondrial p53-dependent pathway and Bax activation, and demonstrate for the first time that AT and NBS T-cells are characterised by almost undetectable mitochondrial p53 accumulation, an altered p53 ubiquitination pattern and increased Mdm2 accumulation. These findings open new perspectives in understanding the multifaceted function of ATM and NBS1 in regulating apoptotic pathways.

2. Material and methods

2.1 Cell isolation, cell culture and drug treatment

Peripheral blood from four healthy donors, three AT and two NBS patients was collected after signed informed consent. AT patients were either homozygous or compound heterozygous for truncating mutations; NBS patients were homozygous for the common 657del5 mutation. PBMC were isolated and T-cell lines, generated as described [42], were maintained by periodic stimulation with PHA (Gibco-Invitrogen, Paisley, UK) and irradiated allogeneic PBMC in complete RPMI medium (RPMI 1640 added with 1% Kanamycin, 1% Sodium Piruvate, 1% L-Glutamine, 1% non essential amino acids, 0.1% β-mercapto-ethanol) (all from Gibco-Invitrogen), supplemented with 5% human serum (BioWitthaker, Cambrex, Baltimore, MD, USA) and 200 U/ml recombinant IL2 (from the myeloma producing cell line IL2-t6, kindly provided by Dr A. Lanzavecchia, IRB, Bellinzona, Switzerland). All experiments were conducted on resting T cells (>95% in G0/G1). The Jurkat human leukemia cell line was purchased from the American Type Culture Collection (Rockville, MD, USA), and grown in complete RPMI medium supplemented with 10% heat-inactivated fetal bovine serum (Gibco, Invitrogen). ActD was supplied by Sigma–Aldrich Co. (St.

Luis, MO, USA) and used at doses ranging from 0.05 to 0.5 μg/ml. Cultured T cells were γ-irradiated (2 Gy) using a 6 MV accelerator (Elekta) at a dose of 2 Gy/min. α-pifithrin (α-PFT) and μ-pifithrin (μ-PFT) (Sigma-Aldrich Co.) were used at 30 μM and 10 μM respectively, and added 20 minutes before ActD. Leptomycin B (LMB) (Applichem, Germany) was used at 10 nM and added 30 minutes before ActD.

2.2 Flow cytometry

Cell viability was determined by propidium iodide (PI) (Sigma-Aldrich Co.) staining; PI was used at the final concentration of 1 μg/ml and maintained at room temperature for 15 min in the dark before the analysis. Cell survival was expressed after normalization to medium alone or supplemented with the drug's solvent (DMSO). Apoptosis was defined through double staining with anti-annexinV-FITC (BD PharMingen, San Diego, CA, USA) and PI, in accordance with the manufacturer's instructions. Caspase activation was analyzed with anti-Active Caspase-3 (BD PharMingen) as primary antibody and a PE-conjugated goat anti-rabbit (BD PharMingen) as secondary antibody, using the Cytofix/Cytoperm Kit (BD PharMingen). Stained cells were analysed on a FACScan (Becton Dikinson & Co., San Jose CA, USA). Statistical analysis of cell survival and caspase-3 activation was performed with either the test of independence or the Student's *t*-test. The significance were expressed in the figures with the asterisks: * $p<0.05$; ** $p<0.01$; *** $p<0.005$.

2.3 Gene silencing by siRNA

The Amaxa Nucleofector system (Lonza, Cologne, Germany) and Amaxa Human T-cell Nucleofector kit were used for electroporation. Briefly, T-cells were resuspended in Nucleofector Solution, Scramble (ON-TARGET Non targeting pool, Thermo Scientific, Rockford, IL, USA) or p53 specific (ON-TARGETplus SMART pool, Human TP53, Thermo Scientific) siRNA oligos (30pmol) were added to $6x10^6$ T-cells/100 μL transfection buffer and nucleofected using the Amaxa Nucleofector II Device and program V-024, according to the manufacturer's instructions. Nucleofected T-cells were maintained in fresh medium for 48 hours, then either treated with ActD for 24 hours or left untreated. Treated and untreated cells were harvested at the same time point.

2.4 Immunofluorescence

Approximately 400,000 T-cells for each condition were collected, fixed with 4% paraformaldehyde, permeabilized with 0.5% Triton X-100, and blocked with 6% bovine serum albumin and 2.5% normal goat serum. They were stained with anti-p53 (clone DO1), anti-BAX (clone 2D2), anti-

Mdm2 (clone H221) specific Abs (all from Santa Cruz Biotechnology, Santa Cruz, CA, USA), and with Alexa 546-conjugated goat anti-mouse as secondary Ab (Molecular Probes, Invitrogen). Green Fluorescent Mitotraker (Molecular Probes, Invitrogen) was used at the final concentration of 100nM. Stained cells were transferred to poly-L-lysine-coated coverslips and slides were mounted with Mowiol (Calbiochem, San Diego, CA, USA). Fluorescence images were obtained with a 510 Carl Zeiss confocal laser microscope using a ×63 objective. Colocalization analyses were performed with LSM510 Image examiner software from Zeiss, selecting the cytosolic area of 20 different cells for each condition, in two independent experiments. Fluorescence intensity analysis was performed with Image examiner software from Zeiss, selecting 20 different cells for each condition elaborated as arbitrary units/pixel. Statistical analysis of fluorescence intensity was performed with the Student's *t*-test. The significance were expressed in the figure with the asterisks: * $p<0.05$; ** $p<0.01$.

2.5 Cell extracts and subcellular fractionation

Cells were harvested and washed with PBS, pelleted, and lysed in Laemmli buffer (0.125 M Tris-HCl [pH 6.8], 5% SDS) containing as inhibitors 1 mM phenylmethylsulfonyl fluoride, pepstatin (10 µg/ml), aprotinin (100 KIU/ml), leupeptin (10 µg/ml) and 1 mM sodium orthovanadate (Na_3VO_4) (all from Calbiochem). Total lysates were boiled for 2 min, sonicated, and quantitated by the micro-bicinchoninic acid method (Thermo Scientific). For nuclear protein isolation, cells were harvested and washed with PBS, pelleted and lysed in 10mM Hepes, 10mM KCl, 1,5mM $MgCl_2$, 0.7% NP-40 (all from Sigma-Aldrich) buffer containing protease inhibitors; subsequently, nuclear proteins were isolated with 20mM Hepes, 0.42 M NaCl, 1,5 mM $MgCl_2$, 0.2 mM EDTA, 25% Glycerol (all from Sigma-Aldrich) buffer containing protease inhibitors and quantitated by the micro-bicinchoninic acid method (Thermo Scientific) before analysis by immunoblotting. For subcellular fractionation, $2x10^7$ T-cells were harvested and washed with PBS; mitochondrial and cytosolic fractions were isolated with the use of the Mitochondria Isolation Kit for cultured cells (Thermo Scientific, reagent-based method). The mitochondrial pellet was lysed in Laemmli buffer, and the cytosolic supernatant was concentrated with a Microcon device (size cut-off 10 kDa) (Millipore Corporation, Bedford, MA, USA). Both fractions were quantitated by the micro-bicinchoninic acid method (Thermo Scientific) before analysis by immunoblotting.

2.6 Immunoblot analysis

40 μg of total lysates and 20 μg of nuclear, mitochondrial and cytosolic fractions were size fractionated by SDS-PAGE 7 to 10% gels and electroblotted onto polyvinylidene difluoride membranes (Amersham, GE Healthcare, Buckinghamshhire, UK). After blocking with 5% nonfat dried milk in PBS plus 0.1% Tween (Sigma-Aldrich Co.), the membranes were incubated with anti-p53 (clone DO7) (YLEM, Avezzano, Italy) , -Tom40 (H-300), -lamin A (H-102), -Mdm2 (H-221) (Santa Cruz Biotechnology), -vinculin (clone hVIN-1), -β-actin (clone AC-72) (Sigma-Aldrich Co.) specific Abs, and subsequently with peroxidase-conjugated secondary antibodies (Amersham, GE Healthcare). The immunoreactive bands were visualized by ECL Super Signal (Thermo Scientific) on autoradiographic films. Autoradiographic bands were scanned and quantified by Kodak 1D Image Analysis Software. p53 mono-ubiquitination was assessed through long exposures of p53 immunoblots to evaluate the appearance of a signal in the range between 60kDa (one p53 monoubiquitylated site) and 120kDa (all eight p53 monoubiquitylated sites), as described [17, 43].

3 Results

3.1. T-cells from AT and NBS patients are resistant to a non-redundant p53-dependent apoptotic pathway induced by ActD

To clarify the mechanism that makes AT and NBS T-cells resistant to ActD-induced apoptosis, we explored the death events initiated by ActD. Control cells harvested 15 hr after ActD treatment did not display any appreciable signs of apoptosis (data not shown), whereas after 24 hr there was an evident increase in the fraction of active caspase-3-positive and annexin V-positive/PI-negative, i.e. early apoptotic, cells (Fig. 1A and 1B). By contrast, similarly treated AT and NBS T-cells completely lacked caspase-3 activation, and were defective in phosphatidylserine translocation from the inner to the outer leaflet of the membrane (Fig. 1A and 1B).

As in our previous study [1], control T-cells treated with ActD accumulated high amounts of total p53 (Fig. 1C). To determine whether p53 contributed to the stress response elicited by ActD, we examined the response of the p53-null Jurkat T-cell line [44]. Our western blot analysis confirmed that p53 was not expressed in Jurkat cells, even after ActD treatment (Fig. 1C). As shown in figure 1D, they were resistant to ActD-induced apoptosis. Their viability at 72h was more than 60% (Jurkat versus control cells: $p<0.0001$ with the test of independence), similar to AT and NBS T-cells [1], and were neither active caspase-3-positive nor AnnexinV-positive/PI-negative at 24 hr (Fig. 1A and B). As a second way to assess the p53 dependence of ActD-activated apoptotic pathway, we depleted p53 by siRNA in control T-cell lines. Immunoblot analysis confirmed that p53 levels decreased after p53 siRNA nucleofection (Fig 1E). We found that p53 knockdown

significantly increased survival (Fig.1F) and decreased caspase-3 activation (Fig 1G) following ActD treatment, further suggesting that p53 is required to activate ActD apoptotic pathway.
These findings support the conclusion that ActD induces a p53-dependent apoptotic pathway in normal T-cells, and that the resistance of AT and NBS T-cells to ActD-induced apoptosis is due to its defective activation.

3.2. Defective ActD-induced p53 cytoplasmic accumulation and Bax activation in AT and NBS T-cells

The similar apoptotic defects observed in AT and NBS T-cells and in p53-deficient Jurkat T-cells prompted us to look for defective p53 accumulation by AT and NBS T-cells following ActD treatment. Surprisingly, their total p53 protein level after 6 hr was only slightly reduced to 78% and 98% of that in control T-cells in AT and NBS T-cells respectively (Fig. 2A), whereas p53 accumulation induced by IR was clearly defective (about 10% and 28% that of control T-cells respectively), as assessed by both western blot analysis [36] and confocal microscopy (Figure 2D), as already reported [37-39].
We thus employed cell fractionation and immunoblot analysis in a more detailed search for major defects in p53 subcellular localization in control, AT and NBS T-cells 6 hours after ActD-treatment. The p53 detected in nuclear extracts from the patients was only slightly defective, being about 81% in AT and 77% in NBS cells compared to the controls (Fig. 2B). In addition, p53 was clearly visible in both the cytosol and the mitochondria of the controls, whereas its accumulation was highly defective in the cytosolic fraction of AT and NBS T-cells (about 20% in AT and 22% in NBS compared to the controls), and nearly undetectable in their mitochondrial fraction (about 6% in AT and 16% in NBS compared to the controls) (Fig. 2C).
The distribution of p53 was then determined by immunfluorescence staining and confocal microscopy with a cytosolic probe (Mitotraker green) in conjunction with the anti-p53 antibody (red). In control T-cells p53 was not only present in the nucleus, but also in the cytosol 6 hr after ActD, as highlighted by the yellow signal in the double-staining with the cytosolic probe (Fig. 2D). In AT and NBS T-cells, on the contrary, p53 nuclear accumulation alone was evident at the same time point (Fig. 2D). Colocalization analysis confirmed these data: p53 was present in about 40% of the cytosolic area of ActD-treated normal T-cells, but in less than 5% of ActD-treated patients' T-cells (data not shown). After 2 Gy IR, a genotoxic stimulus that does not induce apoptosis in resting T-cells [1], p53 was exclusively nuclear in both control and patients' T-cells (Fig. 2D).
Cytosolic accumulation of p53 directly activates Bax to insert and oligomerize into the mitochondrial membrane, thus leading to the cascade of mitochondria-mediated apoptosis and

caspase-3 activation [13]. We therefore sought to find out whether high cytosolic p53 levels in ActD-treated cells were coupled with Bax activation. We monitored Bax distribution by immunofluorescence and confocal microscopy at 9-15-24 hours. In the control T-cells, Bax's baseline cytosolic distribution remained until 15 hr after ActD, when a dot-like pattern was displayed by about 30% of these cells; this value increased to 35% at 24 hr, concomitant with the beginning of apoptosis (Fig. 2E and data not shown). When treated AT cells were examined, no changes in this baseline distribution were detected. In NBS cells, Bax was activated at significantly lower levels than in the controls (6% of positive cells at 24 hr) (Fig. 2E).

These results suggested that cytoplasmic p53 accumulation and changes in Bax distribution are involved in ActD-induced apoptosis, and that this extra-nuclear accumulation and Bax activation are defective in AT cells and, to a lesser extent, in NBS cells.

3.3. ActD-induced apoptosis is dependent on the mitochondrial targeting of p53 from an extranuclear pool

To clarify the role of p53 in ActD-induced apoptosis, we used pharmacological manipulations to distinguish its nuclear and mitochondrial functions. Control T-cells were preincubated with two p53 inhibitors that act through different mechanisms: α-pifithrin (α-PFT) reversibly blocks the p53-mediated transactivation of p53-dependent responsive genes [45]; μ-PFT blocks the interaction of p53 with Bcl-xL and Bcl-2, and selectively inhibits p53 translocation to the mitochondria, without affecting its genomic transactivation function [46].

We used 0.5 μg/ml ActD in order to detect any effect of PFT within 24 hr. At longer incubation times, the activity of α-PFT and μ-PFT is partially lost (our data not shown). While the viability level of ActD-treated control T-cells did not change in the presence of α-PFT, preincubation with μ-PFT conferred significant resistance to ActD-induced apoptosis (70% viability at 24 hr) (Fig. 3A). To demonstrate that blockage of mitochondrial p53 increases viability by inhibiting apoptosis, we assessed caspase-3 activation in control T-cells treated with ActD, either alone or in the presence of α-PFT or μ-PFT. μ-PFT preincubation reduced caspase-3 activation by about 86% compared to ActD alone (Fig. 3B), whereas α-PFT treatment had no effect, as expected. These data suggested that ActD-induced apoptosis depends on mitochondrial p53 functions.

To further investigate the origin of mitochondrial translocated p53, a still debated issue [43, 47], we assessed the effects on cell viability during nuclear export blockage induced by treating control T-cells with leptomycin B (LMB), a potent inhibitor of CRM1-mediated p53 nuclear export [48]. ActD was again used at a dose of 0.5 μg/ml to detect any effect of LMB within 24 hr since it is toxic at longer incubation times (our data not shown). The viability and caspase-3 activation of

these control T-cells did not change in the presence of LMB, suggesting that p53 does not need to traffic through the nucleus to activate the mitochondrial apoptosis (Fig 3C and 3D). To confirm these data, we performed immunoblot analysis of p53 accumulation and localization following ActD treatment in the presence of LMB. Cell fractionation experiments showed that cytoplasmic and nuclear p53 pools became independently stabilized upon stress (Fig. 3E).

3.4. ActD-induced p53 mono-ubiquitination at multiple sites is defective in AT and NBS T lymphocytes.

The nuclear versus cytoplasmic effect of p53 are determined by multiple post-translational modifications. Monoubiquitylation of p53 on one or few lysines is the preferred species that translocates to mitochondria in response to stress [17, 43]. We determined the ubiquitylation status of p53 in control, AT and NBS T-cells after ActD treatment. Long exposure of p53 immunoblot revealed an increase of (multi-)monoubiquitylated protein (6.7-fold at 9 hr) in the controls, whereas it was only about 1.4- and 2.9-fold at 9 hr in the AT and NBS cells respectively (Fig. 4A). Since the monoubiquitylated fraction is a function of the total accumulated protein, we normalised this monoubiquitylated p53 form on the total p53 protein level and found that whereas the monoubiquitylated fraction increased by 2.3-fold at 9 hr in the controls, it was only 0.35- and 0.71-fold (i.e., it decreased with respect to total p53) in the AT and NBS cells respectively (data not shown). This defective ubiquitylation may explain the inability of AT and NBS T-cells to induce p53 mitochondrial localization.

To demonstrate the importance of p53 mono-ubiquitination at multiple sites in directing p53 mitochondrial localization, we determined its levels in the extranuclear compartments. Low levels in untreated cytoplasm increased significantly (2.5-fold) upon stress. Mono-ubiquitylated p53 was not found in untreated mitochondria, though some was detected following ActD treatment (Fig. 4B).

We then compared levels of Mdm2, the major E3 ubiquitin-protein ligase, following ActD and after 2 Gy IR (Fig. 2D). In irradiated cells, Mdm2 upregulation occurred at high levels, whereas it was reduced in ActD-treated cells: compared to ActD-treated cells, 6 hours after IR Mdm2 increased by >2 fold (Fig. 4C). These differently induced levels may help to explain the different responses in ActD-treated and irradiated cells, as the low Mdm2 level we observed after ActD could favour p53 mono-ubiquitylation and extranuclear p53 activity. We finally analysed Mdm2 level following ActD in T-cells from AT and NBS patients. Compared to control T-cells, in AT and NBS T-cells the levels of Mdm2 increased 2.0- and 2.3-fold, respectively (Fig. 4D). Mdm2 expression was also analysed by immunfluorescence staining and confocal microscopy. In the control T-cells Mdm2

increment was scarce 6 hr after ActD (Fig. 4E), while conversely, in AT and NBS T-cells the Mdm2 increment was markedly higher at the same time point (Fig. 4E). These data help to explain the poor fraction of p53 mono-ubiquitination at multiple sites observed in AT and NBS cells.

4 Discussion

Our results disclose an undescribed defect in mitochondrial p53 accumulation in AT and NBS T-cells that makes them resistant to apoptosis following ActD treatment. This common defect may depend on reciprocal post-translational regulation between ATM and NBS1 [4, 22-24, 49], and should be listed among the features of AT and NBS cells. Conferring apoptosis resistance, this defect is particularly significant as it may contribute to the genomic instability typical of AT and NBS cells.

Although acute sensitivity to IR and radiomimetic chemicals is considered to be a generalised feature of AT and NBS T-cells, loss of ATM may correlate with tumor resistance to some forms of DNA-damaging chemotherapy (DNA cross-linking agent cisplatin, topoisomerase II inhibitor doxorubicin, fludarabine, cyclophosphamide, chlorambucil) [50, 51]. This chemoresistance phenotype has been postulated as due to prevention of efficient execution of a p53-dependent apoptotic response: in p53 proficient cells, suppression of ATM protected tumors from being killed by genotoxic agents [52]. Defective apoptosis following DNA damaging treatments was also observed in NBS cells, and apoptosis resistance could not be ascribed to differences in p53 phosphorylation and/or stabilization [53]. ATM has also been shown to be the key to the cascade of regulation of p53-mediated neuronal apoptosis following DNA damage: in ATM knockout mice, developing neurons failed to undergo apoptosis following treatment with various genotoxic compounds [54-56] and ATM inactivation was antiapoptotic in differentiated neurons [57]. These data indicate that ATM (and NBS) functions as a molecular “binary switch” that channels the effects of p53 signaling toward apoptosis by controlling its nuclear and cytoplasmic actions. It is tempting to speculate that the defect in mitochondrial p53 accumulation we have now described here in AT and NBS T-cells following ActD treatment may help to explain some of the apoptotic defects previously observed in ATM- and NBS1-deficient cells.

Analysis of p53 expression revealed that treatment with ActD induced high amounts of total p53 and the finding that p53 deficient Jurkat T-cells, as well as p53-silenced normal T-cells, were resistant to ActD-induced apoptosis suggested that this pathway was non-redundant. Aside from nuclear stabilization, ActD caused cytoplasmic p53 accumulation and translocation to mitochondria. To ascertain the relative contribution of nuclear versus mitochondrial p53 to ActD-induced apoptosis, we employed two distinct variants of the chemical p53 inhibitor pifithrin. Pre-treatment

of T cells with μ-PFT markedly decreased ActD-induced caspase-3 activation, while inhibition of the transcriptional arm of p53 with α-PFT failed to protect T-cells from ActD-induced apoptosis. These results suggest that the extranuclear p53 pool may prevail over its nuclear counterpart in mediating cell death. Thus, the transcription independent p53 program was a major contributor to ActD-induced apoptosis in human T-cells and this could be partly explained by the transcriptional inhibitory activity of ActD, which would interfere with transactivating p53 activity.

The origin of mitochondrial translocated p53 is still debated [43, 47]: monoubiquitination of p53 exposes a C-terminal nuclear export sequence and promotes the dissociation of Mdm2, thereby allowing further post-translational modifications of the C-terminal lysines, such as sumoylation, which promote nuclear export of p53 [58]. Interestingly, however, stress-induced increases in cytoplasmic p53 have been primarily attributed to stabilization of existing cytoplasmic p53 pools instead of shuttling of nuclear p53 into the cytoplasm: careful fractionation experiments suggested that both nuclear and cytoplasmic p53 pools were stabilized independently [43, 59]. Using a non-competitive nuclear export blockade (LMB), we found that nuclear p53 export was not required for mitochondrial translocation upon DNA damage. Instead, distinct nuclear and cytoplasmic p53 pools became simultaneously stabilized after ActD treatment. This is consistent with previous observations [13, 43], and indicates that mitochondrially translocated p53 arises from a distinct cytoplasmic pool.

We have also described a role for Bax in the apoptotic pathway induced by ActD. ActD treatment was followed by an evident change in Bax distribution, while confocal microscopy illustrated the appearance of Bax aggregates reflecting Bax oligomerization and mitochondria pore formation [60]. Bax activation was not observed in AT and NBS cells. NBS1-deficient cells have been found to display a defective apoptosis following DNA damage that was not due to altered gene expression, but to a direct role of NBS1 in regulating apoptosis induction by stimulating Bax activation. The same defect was also described in cells expressing NBS1 with a mutation in the ATM phosphorylation sites [61].

How can ATM and NBS1 impact on extranuclear p53 accumulation? The nuclear versus cytoplasmic effects of p53 are determined by multiple post-translational modifications that affect its interaction with other proteins and its biological activities. One of the most substantial modifications is p53 monoubiquitylation, mainly mediated by low Mdm2 activity, that stimulates p53 arrival at the mitochondria; here, p53 is rapidly deubiquitylated by mitochondrial HAUSP, thus generating the apoptotically active non-ubiquitylated p53 [43, 59]. Consistent with a rapid p53 deubiquitylation was our observation of more abundant mono-ubiquitylated p53 in the cytosolic than in the mitochondrial fractions of ActD-treated cells. The regulation of p53 ubiquitylation by

Mdm2 is a rather complex process and ATM has different roles in this process, direct and indirect. ATM directly phosphorylates Mdm2, decreasing its activity and stability of this protein [62, 63]; phosphorylation by ATM also inhibits Mdm2 RING domain oligomerization, and specifically suppresses its action on p53 polyubiquitylation [64]. In addition, ATM mediates indirect phosphorylation of Mdm2 via the c-Alb kinase, which reduces the Mdm2-mediated ubiquitylation [65]. Mdm2 activity is in turn regulated by Mdmx, promoting Mdm2's activity as an E3 ligase of p53. ATM also phosphorylates Mdmx contributing to ubiquitylation and degradation of Mdmx [66]. Finally, ATM phosphorylation of Mdm2 and Mdmx decreases ubiquitin-specific protease HAUSP's binding to Mdm2/MdmX, promoting their proteasomal degradation [67]. Alteration of any of these events could favour changes in the ubiquitylation pattern of p53. Indeed, our comparison of p53 ubiquitylation pattern in normal, AT and NBS T-cells following ActD treatment disclosed a reduced monoubiquitylated p53 fraction in patients' T-cells. This confirms that monoubiquitylation of p53 is regulated by ATM and suggests for the first time that it is also regulated by NBS1, and contributes to the p53-mediated apoptotic pathway activated by ActD. Second, our finding that Mdm2 poorly accumulates in control T-cells treated with ActD treatment is consistent with a role for low Mdm2 level, through its promotion of p53 monoubiquitylation, in the apoptotic pathway thus induced. Third, the increased Mdm2 levels in ActD-treated AT and NBS T-cells provide a mechanistic link to the apoptotic defect observed in patients' T-cells, suggesting that altered Mdm2 regulation by ATM and, for the first time, by NBS1 is responsible for altered ubiquitylation of p53 in AT and NBS cells. It is notable that the amount of Mdm2 in ActD-treated patients' T cells was comparable to that present in irradiated control T cells, where p53 accumulated only in the nucleus and no apoptotis occourred.

Although other ubiquitin ligases, regulated directly or indirectly by ATM after DNA damage, have been involved in p53 regulation [68, 69], they are only capable of mediating its polyubiquitylation by addressing it to proteasome-mediated degradation. The only exception is represented by MLS2, a new E3 ligase described by Kruse and Gu [70], which regulates p53 subcellular localization by monoubiquitylation, without affecting p53 stability. The possibility that this ubiquitin ligase or additional p53 modification can also contribute to p53 localization and activity following ActD treatment cannot be ruled out at the moment.

In conclusion, we provide new insights linking the pro-apoptotic activity of ActD with the mitochondrial translocation of p53 and dependence of this phenomenon on functional ATM and Nbs1. These data might help to explain some of the apoptotic defects previously observed in ATM- and NBS1-deficient cells, and suggest new roles for these two proteins in regulating apoptotic pathways.

Figure legends

Figure 1: *Selective resistance to ActD-induced apoptosis of T-cells from AT and NBS patients.*

(A) Cultured T-cells from one control, one AT and one NBS patient, and Jurkat T-cells were kept for 24 hr in medium alone or with 0.05 μg/ml ActD, then harvested and stained with anti-active caspase-3 antibody. Percentages of active caspase-3^+ cells are indicated.

(B) Cultured T-cells from one control, one AT and one NBS patient and Jurkat T-cells were kept for 24 hr in medium alone or with 0.05 μg/ml ActD, then harvested and stained with anti-annexin V antibody and PI. Percentages of PI^- annexin V^+ cells are indicated.

(C) Western blot analysis of p53 accumulation on control and Jurkat T-cells harvested before or at various times after 0.05 μg/ml ActD treatment. Probing for β-actin checked lanes for protein content.

(D) Cultured T-cells from three controls (◆) and Jurkat T-cells (∗) were kept in medium alone or in medium containing 0.05 μg/ml of ActD, harvested at 24, 48 and 72 hr and analyzed by flow cytometry after staining with PI. Viability is shown as mean±SD of three independent experiments.

(E) Western blot analysis of p53 in control T-cells transfected with either scrambled or p53 siRNA and treated for 24 hr with 0.05 μg/ml ActD. Probing for vinculin checked lanes for protein content.

(F) Control T-cells transfected with either scrambled or p53 siRNA were treated with 0.05 μg/ml ActD and analyzed at 24 hr by PI staining. Data are normalized to survival in medium alone (bars, mean±SD of two independent experiments)

(G) Control T-cells transfected with either scrambled or p53 siRNA were kept for 24 hr in medium alone or with 0.05 μg/ml ActD, harvested and stained with anti-active caspase-3 antibody. Percentages of active caspase-3^+ cells are indicated.

Figure 2: *Defective ActD-induced p53 cytoplasmic accumulation and Bax activation in T-cells from AT and NBS patients.*

(A) Western blot analysis of p53 accumulation on control, AT and NBS T-cells harvested before or at various times after 0.05 μg/ml ActD treatment. Probing for β-actin checked lanes for protein content.

(B) Immunoblotting analysis of nuclear fractions from control, AT and NBS T-cells harvested before (-) or 6 hr after 0.05 μg/ml ActD treatment (+). Probing for vinculin and lamin A checked lanes for protein content and purity of the fractions.

(C) Immunoblotting analysis of cytosolic and mitochondrial fractions from control, AT and NBS T-cells harvested before (-) or 6 hr after 0.05 μg/ml ActD treatment (+). Probing for vinculin and Tom40 checked lanes for protein content and purity of the fractions. One representative experiment out of two is shown.

(D) Confocal analysis of p53 localization. T-cells from one donor, one AT and one NBS patient were harvested before or 6 hr after either 2Gy γ-IR or 0.05 μg/ml ActD and stained with anti-p53 mAb as primary antibody, with Alexa 546-conjugated goat anti-mouse as secondary Ab and with Green Fluorescent Mitotraker. One representative experiment out of three is shown.

(E) Confocal analysis of Bax distribution. Cultured T-cells from one donor, one AT and one NBS patient were harvested before or 15 hr after 0.05 μg/ml ActD and stained with anti-Bax mAb as primary antibody, with Alexa 546-conjugated goat anti-mouse as secondary Ab. One representative experiment out of two is shown.

Figure 3: *Effect of the p53-inhibitors α-PFT and μ-PFT, and of nuclear export blockage on the ActD-induced apoptosis.*

(A) T-cell lines from three healthy donors were treated with either 10μM μ-PFT or 30μM α-PFT alone or in conjunction with 0.5 μg/ml ActD, and analyzed at 24 hr by PI staining. Data are normalized to survival in medium alone (bars, mean±SD of three independent experiment)

(B) T-cell lines from three healthy donors were treated with either 10μM μ-PFT or 30μM α-PFT alone or in conjunction with 0.5 μg/ml ActD, and analyzed at 24 hr with anti-active caspase-3 antibody. Data are normalized to caspase activation with ActD alone (bars, mean±SD of three independent experiment)

(C) T-cell lines from two healthy donors were treated with 10 nM LMB, alone or in conjunction with 0.5 μg/ml ActD, and analyzed at 24 hr by PI staining. Data are normalized to survival in medium alone (bars, mean±SD)

(D) T-cell lines from two healthy donors were treated with either 10 nM LMB, alone or in conjunction with 0.5 μg/ml ActD, and analyzed at 24 hr with anti-active caspase-3 antibody. Data are normalized to caspase activation with ActD alone (bars, mean±SD)

(E) Immunoblotting analysis of p53 accumulation in control T-cells in the presence of LMB. Left panel: T-cells were harvested before (-) or 6 hr after treatment with 0.05 μg/ml ActD, alone or in conjunction with 10 nM LMB, and then analysed for their total protein extract (left panel), nuclear fraction (central panel), and cytosolic and mitochondrial fraction (left panel). Probing for vinculin, lamin-A and Tom40 checked lanes for protein content and purity of the fractions. One representative experiment out of three is shown.

Figure 4: *Defective p53 mono-ubiquitination at multiple sites in AT and NBS T-cells following ActD treatment.*

(A) Immunoblotting analysis of p53 mono-ubiquitination at multiple sites on total protein extract from control, AT and NBS T-cells harvested before or at various times after 0.05 μg/ml ActD treatment. Probing for vinculin checked lanes for protein content. Quantification of p53 mono-ubiquitination at multiple sites is shown as normalized for vinculin content.

(B) Immunoblotting analysis of p53 mono-ubiquitination at multiple sites of mitochondrial and cytosolic fractions from a control T-cell line harvested before (-) or 6 hr after 0.05 μg/ml ActD treatment (+). Probing for vinculin and Tom40 checked lanes for protein content and purity of the fractions. One representative experiment out of two is shown.

(C) Time course analysis of Mdm2 levels on control T-cells harvested before or at various times after either 0.05 μg/ml ActD treatment or 2 Gy gamma irradiation. Probing for β-actin checked lanes for protein content.

(D) Western blot analysis of Mdm2 from control, AT and NBS T-cells harvested before (-) or 6 hours after 0.05 μg/ml ActD treatment (+). Probing for vinculin checked lanes for protein content. Quantification of Mdm2 signal is shown after normalization for vinculin content.

(E) Confocal analysis of Mdm2 levels following ActD treatment. Upper panel: normal, AT and NBS T-cells were harvested before or 6 hr after 0.05 μg/ml ActD treatment and stained with anti-Mdm2 mAb as primary antibody, with Alexa 546-conjugated goat anti-mouse as secondary Ab. A representative experiment out of three is shown. Lower panel: quantification of Mdm2 levels before (-) or 6 hr after 0.05 μg/ml ActD (+) on two control, three AT and two NBS T-cells is shown.

Acknowledgements

The authors thank G. Del Sal, C.I.B., Trieste, Italy for careful critical reading and suggestions and K. Chrzanowska, Children's Memorial Health Institute, Warsaw, Poland, for providing biological samples from NBS patients. This work was partially supported by grants from 'Regione Piemonte' (Ricerca Sanitaria Finalizzata 2008bis and 2009) and from 'Fondazione Enrico, Umberto e Livia Benassi', Turin, Italy, and the Italian Association for Cancer Research (AIRC).

References

[1] P. Porcedda, V. Turinetto, E. Lantelme, E. Fontanella, K. Chrzanowska, R. Ragona, M. De Marchi, D. Delia, C. Giachino, Impaired elimination of DNA double-strand break-containing lymphocytes in ataxia telangiectasia and Nijmegen breakage syndrome, DNA repair, 5 (2006) 904-913.

[2] S.P. Jackson, Sensing and repairing DNA double-strand breaks, Carcinogenesis, 23 (2002) 687-696.
[3] D.C. van Gent, J.H. Hoeijmakers, R. Kanaar, Chromosomal stability and the DNA double-stranded break connection, Nat Rev Genet, 2 (2001) 196-206.
[4] Y. Shiloh, ATM and related protein kinases: safeguarding genome integrity, Nature reviews, 3 (2003) 155-168.
[5] K.L. Cann, G.G. Hicks, Regulation of the cellular DNA double-strand break response, Biochemistry and cell biology = Biochimie et biologie cellulaire, 85 (2007) 663-674.
[6] J.H. Hoeijmakers, DNA damage, aging, and cancer, The New England journal of medicine, 361 (2009) 1475-1485.
[7] C.J. Norbury, B. Zhivotovsky, DNA damage-induced apoptosis, Oncogene, 23 (2004) 2797-2808.
[8] Y. Aylon, M. Oren, Living with p53, dying of p53, Cell, 130 (2007) 597-600.
[9] K.H. Vousden, X. Lu, Live or let die: the cell's response to p53, Nature reviews, 2 (2002) 594-604.
[10] T. Riley, E. Sontag, P. Chen, A. Levine, Transcriptional control of human p53-regulated genes, Nat Rev Mol Cell Biol, 9 (2008) 402-412.
[11] D.R. Green, G. Kroemer, Cytoplasmic functions of the tumour suppressor p53, Nature, 458 (2009) 1127-1130.
[12] M. Mihara, S. Erster, A. Zaika, O. Petrenko, T. Chittenden, P. Pancoska, U.M. Moll, p53 has a direct apoptogenic role at the mitochondria, Molecular cell, 11 (2003) 577-590.
[13] J.E. Chipuk, T. Kuwana, L. Bouchier-Hayes, N.M. Droin, D.D. Newmeyer, M. Schuler, D.R. Green, Direct activation of Bax by p53 mediates mitochondrial membrane permeabilization and apoptosis, Science (New York, N.Y, 303 (2004) 1010-1014.
[14] J.I. Leu, P. Dumont, M. Hafey, M.E. Murphy, D.L. George, Mitochondrial p53 activates Bak and causes disruption of a Bak-Mcl1 complex, Nature cell biology, 6 (2004) 443-450.
[15] J.P. Kruse, W. Gu, Modes of p53 regulation, Cell, 137 (2009) 609-622.
[16] J.C. Marine, G. Lozano, Mdm2-mediated ubiquitylation: p53 and beyond, Cell death and differentiation, 17 93-102.
[17] M. Li, C.L. Brooks, F. Wu-Baer, D. Chen, R. Baer, W. Gu, Mono- versus polyubiquitination: differential control of p53 fate by Mdm2, Science (New York, N.Y, 302 (2003) 1972-1975.
[18] M.F. Lavin, Ataxia-telangiectasia: from a rare disorder to a paradigm for cell signalling and cancer, Nat Rev Mol Cell Biol, 9 (2008) 759-769.
[19] S.G. Becker-Catania, R.A. Gatti, Ataxia-telangiectasia, Advances in experimental medicine and biology, 495 (2001) 191-198.
[20] Y. Shiloh, Ataxia-telangiectasia and the Nijmegen breakage syndrome: related disorders but genes apart, Annual review of genetics, 31 (1997) 635-662.
[21] M. Digweed, K. Sperling, Nijmegen breakage syndrome: clinical manifestation of defective response to DNA double-strand breaks, DNA repair, 3 (2004) 1207-1217.
[22] J.H. Lee, T.T. Paull, Direct activation of the ATM protein kinase by the Mre11/Rad50/Nbs1 complex, Science (New York, N.Y, 304 (2004) 93-96.
[23] J.H. Lee, T.T. Paull, ATM activation by DNA double-strand breaks through the Mre11-Rad50-Nbs1 complex, Science (New York, N.Y, 308 (2005) 551-554.
[24] S. Difilippantonio, A. Nussenzweig, The NBS1-ATM connection revisited, Cell cycle (Georgetown, Tex, 6 (2007) 2366-2370.
[25] H.H. Chun, R.A. Gatti, Ataxia-telangiectasia, an evolving phenotype, DNA repair, 3 (2004) 1187-1196.
[26] I. Kondratenko, O. Paschenko, A. Polyakov, A. Bologov, Nijmegen breakage syndrome, Advances in experimental medicine and biology, 601 (2007) 61-67.

[27] C. Knorr, T. Meyer, T. Janssen, J. Goehl, W. Hohenberger, Hyperthermic isolated limb perfusion (HILP) in malignant melanoma. Experience with 101 patients, Eur J Surg Oncol, 32 (2006) 224-227.
[28] D.M. Green, C.A. Cotton, M. Malogolowkin, N.E. Breslow, E. Perlman, J. Miser, M.L. Ritchey, P.R. Thomas, P.E. Grundy, G.J. D'Angio, J.B. Beckwith, R.C. Shamberger, G.M. Haase, M. Donaldson, R. Weetman, M.J. Coppes, P. Shearer, P. Coccia, M. Kletzel, R. Macklis, G. Tomlinson, V. Huff, R. Newbury, D. Weeks, Treatment of Wilms tumor relapsing after initial treatment with vincristine and actinomycin D: a report from the National Wilms Tumor Study Group, Pediatric blood & cancer, 48 (2007) 493-499.
[29] M. Moschovi, G. Trimis, K. Stefanaki, J. Anastasopoulos, V. Syriopoulou, E. Koultouki, F. Tzortzatou-Stathopoulou, Favorable outcome of Ewing sarcoma family tumors to multiagent intensive preoperative chemotherapy: a single institution experience, Journal of surgical oncology, 89 (2005) 239-243.
[30] K.M. Tewey, T.C. Rowe, L. Yang, B.D. Halligan, L.F. Liu, Adriamycin-induced DNA damage mediated by mammalian DNA topoisomerase II, Science (New York, N.Y, 226 (1984) 466-468.
[31] R.P. Perry, D.E. Kelley, Inhibition of RNA synthesis by actinomycin D: characteristic dose-response of different RNA species, Journal of cellular physiology, 76 (1970) 127-139.
[32] M.J. Miller, Sensitivity of RNA synthesis to actinomycin D inhibition is dependent on the frequency of transcription: a mathematical model, Journal of theoretical biology, 129 (1987) 289-299.
[33] Y. Sedletska, M.J. Giraud-Panis, J.M. Malinge, Cisplatin is a DNA-damaging antitumour compound triggering multifactorial biochemical responses in cancer cells: importance of apoptotic pathways, Current medicinal chemistry, 5 (2005) 251-265.
[34] J.A. Holden, DNA topoisomerases as anticancer drug targets: from the laboratory to the clinic, Current medicinal chemistry, 1 (2001) 1-25.
[35] A. Motegi, Y. Murakawa, S. Takeda, The vital link between the ubiquitin-proteasome pathway and DNA repair: impact on cancer therapy, Cancer letters, 283 (2009) 1-9.
[36] V. Turinetto, P. Porcedda, L. Orlando, M. De Marchi, A. Amoroso, C. Giachino, The cyclin-dependent kinase inhibitor 5, 6-dichloro-1-beta-D-ribofuranosylbenzimidazole induces nongenotoxic, DNA replication-independent apoptosis of normal and leukemic cells, regardless of their p53 status, BMC cancer, 9 (2009) 281.
[37] K.K. Khanna, M.F. Lavin, Ionizing radiation and UV induction of p53 protein by different pathways in ataxia-telangiectasia cells, Oncogene, 8 (1993) 3307-3312.
[38] W. Jongmans, M. Vuillaume, K. Chrzanowska, D. Smeets, K. Sperling, J. Hall, Nijmegen breakage syndrome cells fail to induce the p53-mediated DNA damage response following exposure to ionizing radiation, Molecular and cellular biology, 17 (1997) 5016-5022.
[39] N. Nasrin, M. Kunhi, M. Einspenner, S. al-Sedairy, M. Hannan, Reduced induction of P53 protein by gamma-irradiation in ataxia telangiectasia cells without constitutional mutations in exons 5, 6, 7, and 8 of the p53 gene, Cancer genetics and cytogenetics, 77 (1994) 14-18.
[40] E. Riballo, M. Kuhne, N. Rief, A. Doherty, G.C. Smith, M.J. Recio, C. Reis, K. Dahm, A. Fricke, A. Krempler, A.R. Parker, S.P. Jackson, A. Gennery, P.A. Jeggo, M. Lobrich, A pathway of double-strand break rejoining dependent upon ATM, Artemis, and proteins locating to gamma-H2AX foci, Molecular cell, 16 (2004) 715-724.
[41] P. Jeggo, M.F. Lavin, Cellular radiosensitivity: how much better do we understand it?, International journal of radiation biology, 85 (2009) 1061-1081.
[42] E. Lantelme, B. Palermo, L. Granziero, S. Mantovani, R. Campanelli, V. Monafo, A. Lanzavecchia, C. Giachino, Cutting edge: recombinase-activating gene expression and V(D)J recombination in CD4+CD3low mature T lymphocytes, J Immunol, 164 (2000) 3455-3459.
[43] N.D. Marchenko, S. Wolff, S. Erster, K. Becker, U.M. Moll, Monoubiquitylation promotes mitochondrial p53 translocation, The EMBO journal, 26 (2007) 923-934.

[44] J. Cheng, M. Haas, Frequent mutations in the p53 tumor suppressor gene in human leukemia T-cell lines, Molecular and cellular biology, 10 (1990) 5502-5509.
[45] P.G. Komarov, E.A. Komarova, R.V. Kondratov, K. Christov-Tselkov, J.S. Coon, M.V. Chernov, A.V. Gudkov, A chemical inhibitor of p53 that protects mice from the side effects of cancer therapy, Science (New York, N.Y, 285 (1999) 1733-1737.
[46] E. Strom, S. Sathe, P.G. Komarov, O.B. Chernova, I. Pavlovska, I. Shyshynova, D.A. Bosykh, L.G. Burdelya, R.M. Macklis, R. Skaliter, E.A. Komarova, A.V. Gudkov, Small-molecule inhibitor of p53 binding to mitochondria protects mice from gamma radiation, Nature chemical biology, 2 (2006) 474-479.
[47] P. Dumont, J.I. Leu, A.C. Della Pietra, 3rd, D.L. George, M. Murphy, The codon 72 polymorphic variants of p53 have markedly different apoptotic potential, Nature genetics, 33 (2003) 357-365.
[48] T.R. Shirangi, A. Zaika, U.M. Moll, Nuclear degradation of p53 occurs during down-regulation of the p53 response after DNA damage, Faseb J, 16 (2002) 420-422.
[49] M.F. Lavin, S. Kozlov, N. Gueven, C. Peng, G. Birrell, P. Chen, S. Scott, Atm and cellular response to DNA damage, Advances in experimental medicine and biology, 570 (2005) 457-476.
[50] L. Ripolles, M. Ortega, F. Ortuno, A. Gonzalez, J. Losada, J. Ojanguren, J.A. Soler, J. Bergua, M.D. Coll, M.R. Caballin, Genetic abnormalities and clinical outcome in chronic lymphocytic leukemia, Cancer genetics and cytogenetics, 171 (2006) 57-64.
[51] B. Austen, A. Skowronska, C. Baker, J.E. Powell, A. Gardiner, D. Oscier, A. Majid, M. Dyer, R. Siebert, A.M. Taylor, P.A. Moss, T. Stankovic, Mutation status of the residual ATM allele is an important determinant of the cellular response to chemotherapy and survival in patients with chronic lymphocytic leukemia containing an 11q deletion, J Clin Oncol, 25 (2007) 5448-5457.
[52] H. Jiang, H.C. Reinhardt, J. Bartkova, J. Tommiska, C. Blomqvist, H. Nevanlinna, J. Bartek, M.B. Yaffe, M.T. Hemann, The combined status of ATM and p53 link tumor development with therapeutic response, Genes & development, 23 (2009) 1895-1909.
[53] N. Thierfelder, I. Demuth, N. Burghardt, K. Schmelz, K. Sperling, K.H. Chrzanowska, E. Seemanova, M. Digweed, Extreme variation in apoptosis capacity amongst lymphoid cells of Nijmegen breakage syndrome patients, European journal of cell biology, 87 (2008) 111-121.
[54] M.R. Macleod, L. Ramage, A. McGregor, J.R. Seckl, Reduced NMDA-induced apoptosis in neurons lacking ataxia telangiectasia mutated protein, Neuroreport, 14 (2003) 215-217.
[55] Y. Lee, M.J. Chong, P.J. McKinnon, Ataxia telangiectasia mutated-dependent apoptosis after genotoxic stress in the developing nervous system is determined by cellular differentiation status, J Neurosci, 21 (2001) 6687-6693.
[56] E. Keramaris, A. Hirao, R.S. Slack, T.W. Mak, D.S. Park, Ataxia telangiectasia-mutated protein can regulate p53 and neuronal death independent of Chk2 in response to DNA damage, The Journal of biological chemistry, 278 (2003) 37782-37789.
[57] L.J. Martin, Z. Liu, J. Pipino, B. Chestnut, M.A. Landek, Molecular regulation of DNA damage-induced apoptosis in neurons of cerebral cortex, Cereb Cortex, 19 (2009) 1273-1293.
[58] S. Carter, O. Bischof, A. Dejean, K.H. Vousden, C-terminal modifications regulate MDM2 dissociation and nuclear export of p53, Nature cell biology, 9 (2007) 428-435.
[59] N.D. Marchenko, U.M. Moll, The role of ubiquitination in the direct mitochondrial death program of p53, Cell cycle (Georgetown, Tex, 6 (2007) 1718-1723.
[60] M.G. Annis, E.L. Soucie, P.J. Dlugosz, J.A. Cruz-Aguado, L.Z. Penn, B. Leber, D.W. Andrews, Bax forms multispanning monomers that oligomerize to permeabilize membranes during apoptosis, The EMBO journal, 24 (2005) 2096-2103.
[61] K. Iijima, C. Muranaka, J. Kobayashi, S. Sakamoto, K. Komatsu, S. Matsuura, N. Kubota, H. Tauchi, NBS1 regulates a novel apoptotic pathway through Bax activation, DNA repair, 7 (2008) 1705-1716.

[62] R. Maya, M. Balass, S.T. Kim, D. Shkedy, J.F. Leal, O. Shifman, M. Moas, T. Buschmann, Z. Ronai, Y. Shiloh, M.B. Kastan, E. Katzir, M. Oren, ATM-dependent phosphorylation of Mdm2 on serine 395: role in p53 activation by DNA damage, Genes & development, 15 (2001) 1067-1077.
[63] E. Meulmeester, Y. Pereg, Y. Shiloh, A.G. Jochemsen, ATM-mediated phosphorylations inhibit Mdmx/Mdm2 stabilization by HAUSP in favor of p53 activation, Cell cycle (Georgetown, Tex, 4 (2005) 1166-1170.
[64] Q. Cheng, L. Chen, Z. Li, W.S. Lane, J. Chen, ATM activates p53 by regulating MDM2 oligomerization and E3 processivity, The EMBO journal, 28 (2009) 3857-3867.
[65] Z. Goldberg, R. Vogt Sionov, M. Berger, Y. Zwang, R. Perets, R.A. Van Etten, M. Oren, Y. Taya, Y. Haupt, Tyrosine phosphorylation of Mdm2 by c-Abl: implications for p53 regulation, The EMBO journal, 21 (2002) 3715-3727.
[66] Y. Pereg, D. Shkedy, P. de Graaf, E. Meulmeester, M. Edelson-Averbukh, M. Salek, S. Biton, A.F. Teunisse, W.D. Lehmann, A.G. Jochemsen, Y. Shiloh, Phosphorylation of Hdmx mediates its Hdm2- and ATM-dependent degradation in response to DNA damage, Proceedings of the National Academy of Sciences of the United States of America, 102 (2005) 5056-5061.
[67] E. Meulmeester, M.M. Maurice, C. Boutell, A.F. Teunisse, H. Ovaa, T.E. Abraham, R.W. Dirks, A.G. Jochemsen, Loss of HAUSP-mediated deubiquitination contributes to DNA damage-induced destabilization of Hdmx and Hdm2, Molecular cell, 18 (2005) 565-576.
[68] D. Dornan, H. Shimizu, A. Mah, T. Dudhela, M. Eby, K. O'Rourke, S. Seshagiri, V.M. Dixit, ATM engages autodegradation of the E3 ubiquitin ligase COP1 after DNA damage, Science (New York, N.Y, 313 (2006) 1122-1126.
[69] Q. Li, S. Lin, X. Wang, G. Lian, Z. Lu, H. Guo, K. Ruan, Y. Wang, Z. Ye, J. Han, S.C. Lin, Axin determines cell fate by controlling the p53 activation threshold after DNA damage, Nature cell biology, 11 (2009) 1128-1134.
[70] J.P. Kruse, W. Gu, MSL2 promotes Mdm2-independent cytoplasmic localization of p53, The Journal of biological chemistry, 284 (2009) 3250-3263.

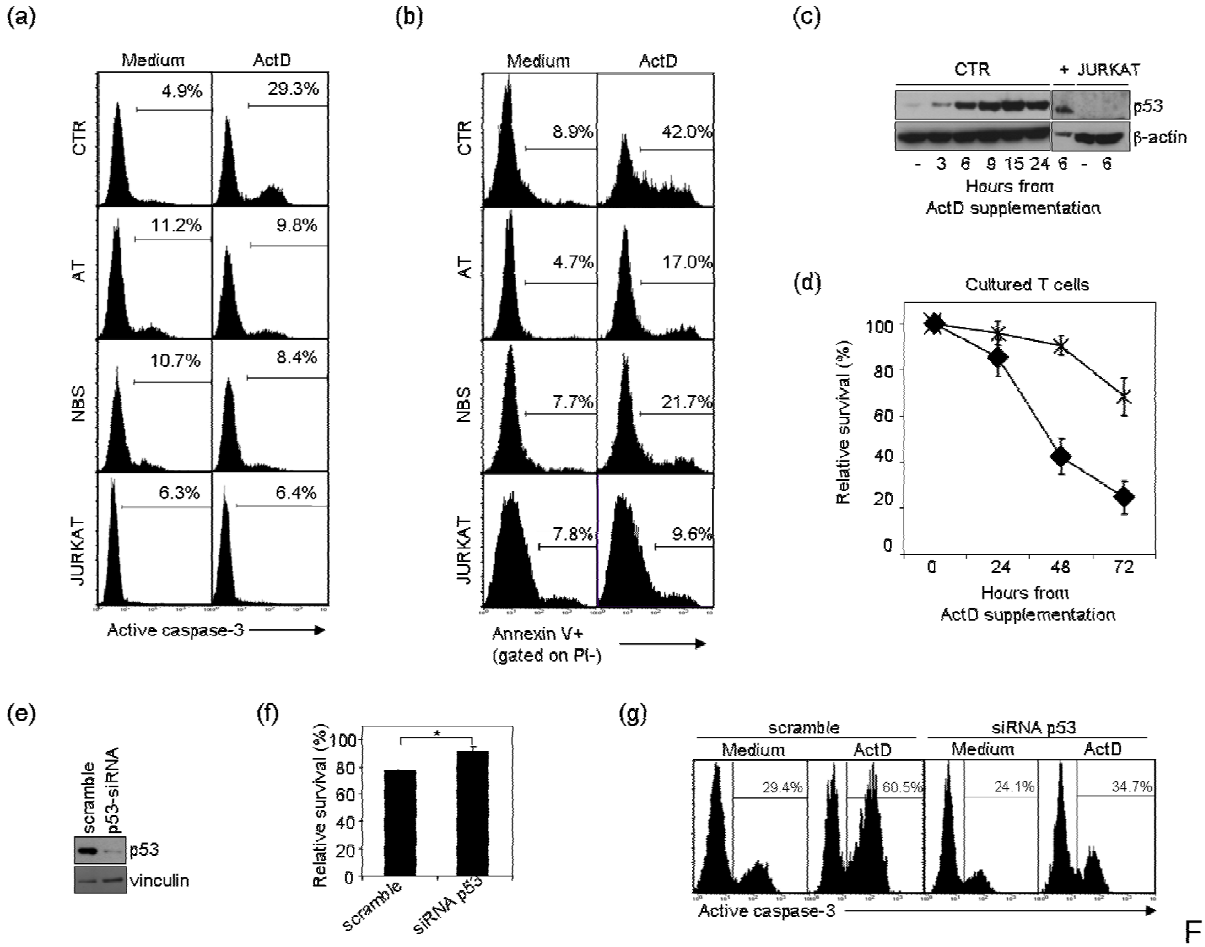
(a)
Medium
ActD
CTR
AT
NBS
JURKAT
4.9%
29.3%
11.2%
9.8%
10.7%
8.4%
6.3%
6.4%
Active caspase-3
(b)
Medium
ActD
8.9%
42.0%
4.7%
17.0%
7.7%
21.7%
7.8%
9.6%
Annexin V+
(gated on PI-)
(c)
CTR
+ JURKAT
p53
β-actin
- 3 6 9 15 24 6 - 6
Hours from
ActD supplementation
(d)
Cultured T cells
Relative survival (%)
100
80
60
40
20
0
0
24
48
72
Hours from
ActD supplementation
(e)
scramble
p53-siRNA
p53
vinculin
(f)
Relative survival (%)
100
80
60
40
20
0
*
scramble
siRNA p53
(g)
scramble
siRNA p53
Medium
ActD
Medium
ActD
29.4%
60.5%
24.1%
34.7%
Active caspase-3

Fig. 1

(a)

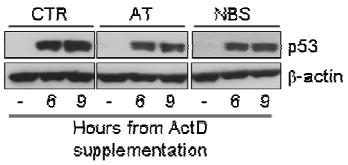
CTR
AT
NBS
p53
β-actin
- 6 9 - 6 9 - 6 9
Hours from ActD supplementation

(b)

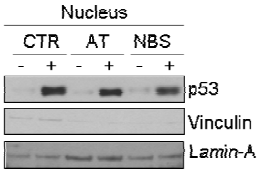
Nucleus
CTR AT NBS
- + - + - +
p53
Vinculin
Lamin-A

(c)

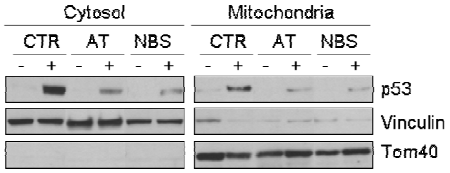
Cytosol
Mitochondria
CTR AT NBS CTR AT NBS
- + - + - + - + - + - +
p53
Vinculin
Tom40

(d)

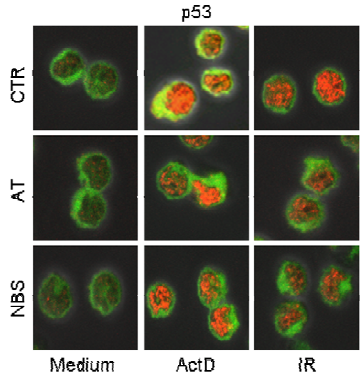
p53
CTR
AT
NBS
Medium
ActD
IR

(e)

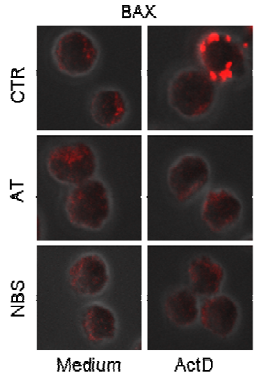
BAX
CTR
AT
NBS
Medium
ActD

Fig. 2

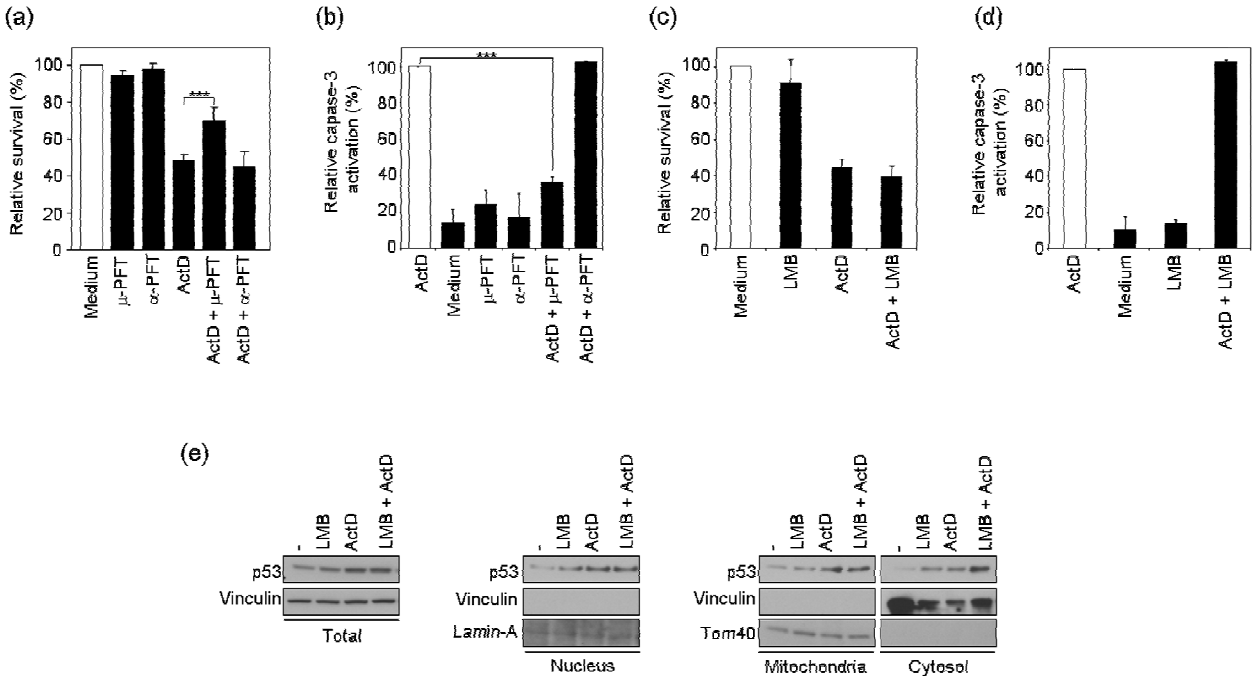
(a)
Relative survival (%)
100
80
60
40
20
0
***
Medium
μ-PFT
α-PFT
ActD
ActD + μ-PFT
ActD + α-PFT
(b)
Relative capase-3 activation (%)
100
80
60
40
20
0
***
ActD
Medium
μ-PFT
α-PFT
ActD + μ-PFT
ActD + α-PFT
(c)
Relative survival (%)
100
80
60
40
20
0
Medium
LMB
ActD
ActD + LMB
(d)
Relative capase-3 activation (%)
100
80
60
40
20
0
ActD
Medium
LMB
ActD + LMB
(e)
-
LMB
ActD
LMB + ActD
p53
Vinculin
Total
-
LMB
ActD
LMB + ActD
p53
Vinculin
Lamin-A
Nucleus
-
LMB
ActD
LMB + ActD
p53
Vinculin
Tom40
Mitochondria
-
LMB
ActD
LMB + ActD
Cytosol

Fig. 3

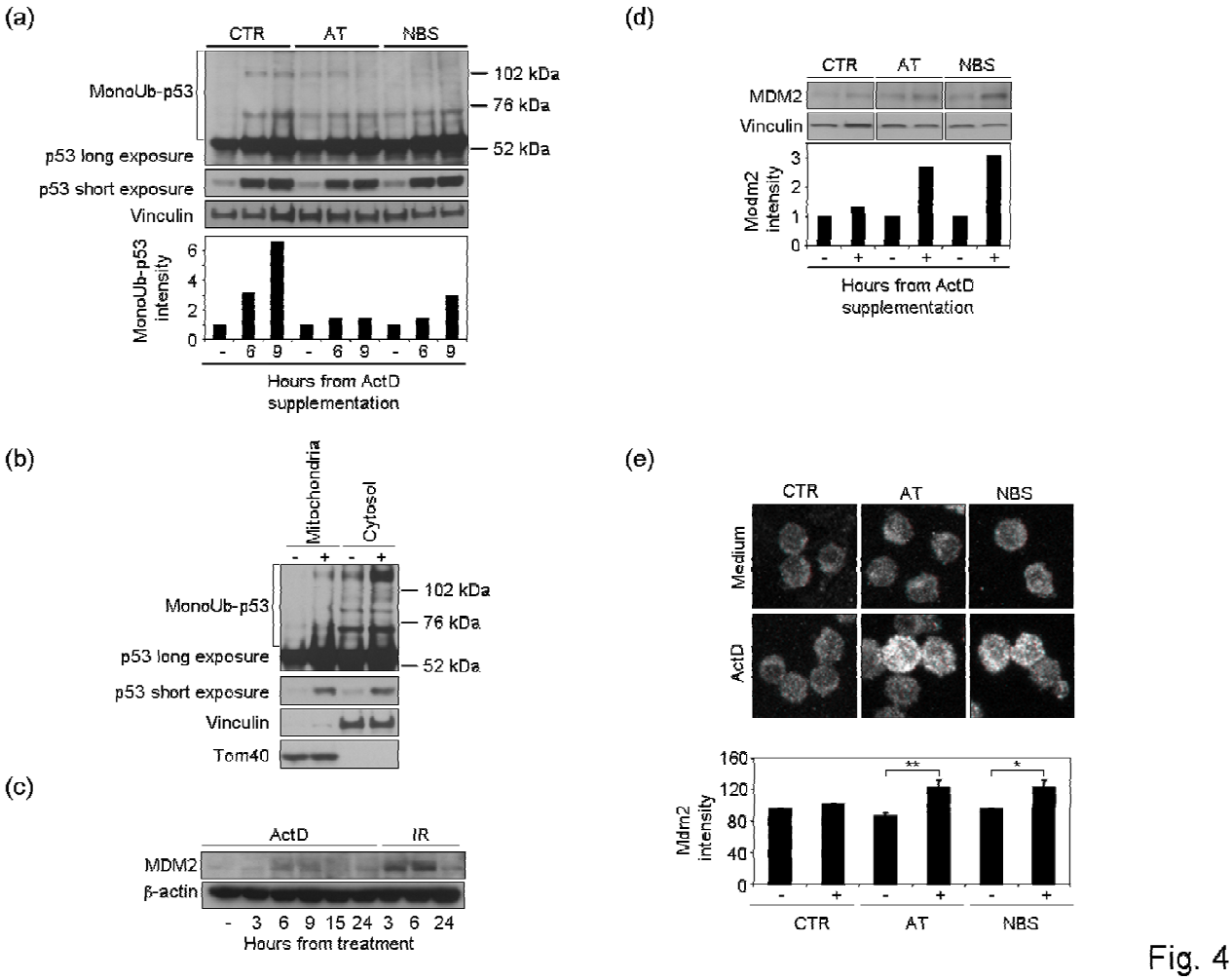
(a)
CTR
AT
NBS
MonoUb-p53
p53 long exposure
p53 short exposure
Vinculin
102 kDa
76 kDa
52 kDa
MonoUb-p53 intensity
Hours from ActD supplementation
(b)
Mitochondria
Cytosol
MonoUb-p53
p53 long exposure
p53 short exposure
Vinculin
Tom40
102 kDa
76 kDa
52 kDa
(c)
ActD
IR
MDM2
β-actin
Hours from treatment
(d)
CTR
AT
NBS
MDM2
Vinculin
Modm2 intensity
Hours from ActD supplementation
(e)
CTR
AT
NBS
Medium
ActD
Mdm2 intensity

Fig. 4